ISSN 1392-1207. MECHANIKA. Vol. 30, No. 6, 2024: 560–567

Optimization of Tensile Strength in AA6063 Friction Stir Welds using ANOVA and ANFIS: A Statistical Analysis of Process Parameters

Deepika MISHRA*, Ravi Shankar PRASAD, Sudhir KUMAR*****
**Jaypee University, Department of Mechanical Engineering, Anoopshahr 203390, India,*
E-mail: deepmish981@gmail.com
***Amrapali University, Department of Mechanical Engineering, Haldwani 263139, India, E-mail: ravp077@gmail.com*
****HIMT Group of Institutions, Department of Mechanical Engineering, Greater Noida (UP) 201310, India,*
E-mail: s_k_tomar02@yahoo.com

https://doi.org/10.5755/j02.mech.33779

1. Introduction

The demand for joining thick aluminum alloys has significantly increased in industries such as aerospace, defense, transportation, and shipbuilding, due to the need for strong, durable joints [1]. Achieving high surface quality and mechanical strength in thick aluminum alloys poses a challenge for traditional fusion welding methods [2]. Friction stir welding (FSW) has emerged as an ideal alternative, offering a green, efficient welding process [3, 4]. In FSW, a rotating tool moves along the metal plate, generating frictional heat that softens the material, allowing the two plates to plastically deform and join together [5]. The softer material moves toward the advancing side due to higher friction, while the lower temperature on the trailing side results in less movement, leading to solid-state bonding of the plates [6].

However, thick materials behave differently compared to thin ones in FSW, often causing the plates to swell significantly, necessitating a redesign of the process. The tool pin shoulder rise (*TPSR*) has proven to be a critical process parameter for joining thick aluminum plates effectively [7, 8]. Optimizing this parameter, along with spindle speed and tool pin length, is essential for ensuring high-quality joints [9]. Process optimization techniques such as regression analysis, response surface methods, and Analysis of Variance (ANOVA) have been employed to improve joint strength while reducing errors and resource usage [10]. Among these, the Taguchi design of experiment (DoE) method, based on orthogonal arrays, has gained prominence for its ability to streamline the optimization process. By combining Taguchi with ANOVA, researchers can estimate the influence of input parameters on output variables, improving the overall process [11, 12, 13].

Studies have shown that spindle speed is the most influential factor in determining tensile strength, accounting for 23% of the effect, while welding speed has a lesser impact at 16% [14, 15]. Through DoE methods like the L9 orthogonal array, the number of experiments required for optimization can be minimized without compromising accuracy [16]. In parallel, mathematical models such as ANFIS (Artificial Neuro-Fuzzy Inference System) and regression equations have been developed to predict and optimize process parameters. ANFIS, in particular, has proven effective when paired with advanced optimization techniques like the Harris Hawks algorithm [17]. Experimental and computational models confirm that rotational speed plays a pivotal role in joint strength, and ANFIS models have consistently demonstrated superior accuracy compared to other modeling techniques like Artificial Neural Networks (ANN) [18].

FSW process modeling and optimization for aluminum alloys, especially dissimilar materials, continue to evolve. By adjusting rotational speed, translational speed, and external forces, researchers have developed accurate predictions for tensile strength and ductility [19]. ANFIS-based models, validated through experimental data, provide a reliable approach for optimizing FSW processes, ensuring high-quality welds in thick aluminum alloys [20].

1.1. Innovations in present work

In this study, a novel approach was developed to establish a solid-state joining process for 12 mm thick AA6063 aluminum plates. The welding of such thick plates posed challenges due to significant thermal expansion caused by rising temperatures. A key innovation was the introduction of a new input parameter, tool pin shoulder rise (*TPSR*), which was identified as a critical factor influencing welding quality. Unlike conventional methods for thin plates, the process for thick plates requires a different approach, with *TPSR* playing a pivotal role. Optimization and ANOVA results confirmed that *TPSR* is essential and should be considered a significant parameter for enhancing tensile strength in thick-plate welding processes.

2. Work Methodology

The material for this study, an aluminum alloy plate measuring 102 mm in width and 12 mm in thickness, was sourced from a metal supplier and confirmed as AA6063 through spectro analysis. The quantity of raw material required was carefully calculated, and the experimental process was designed to minimize the number of tests by using the L9 orthogonal array. The results from this method were further compared with data from a full factorial experiment. Plate samples were prepared using an abrasive cutter and angle grinder, while key process parameters—spindle speed *(SS)*, tool pin length *(TPL)*, and tool pin shoulder rise *(TPSR)*—were selected for analysis. These parameter levels were finalized after multiple trial experiments.

The tool material, also tested via spectro analysis, was identified as SS304. The tool profile was then designed and manufactured using a CNC machine. A custom fixture was fabricated to securely mount the samples for welding, allowing for precise measurement of plunging force. A vertical milling center (VMC) was used to conduct the welding

experiments, producing solid-state joints. Tensile test samples were cut using a hand hacksaw and milling machine, then tested using a computerized universal testing machine according to ASTM E8 standards.

Taguchi analysis was employed to identify the optimal input parameters, with Minitab software used to determine the tensile strength for these optimized parameters. A multiple variable regression analysis was performed to develop a mathematical model for predicting tensile strength. Additionally, the process was modeled using ANFIS (Artificial Neuro-Fuzzy Inference System), and the outputs for optimized parameters were compared with both the experimentally obtained data and the regression model predictions. This comprehensive approach enabled a thorough understanding of the FSW process and its key influencing factors.

2.1. Materials and machine tools

The friction stir welding experiments in this study utilized AA6063, an aluminum-based alloy known for its versatility in architectural applications. AA6063 is valued for its ability to be extruded into complex shapes, its excellent surface finish, high corrosion resistance, good weldability, ease of anodization, and good formability [21]. A chemical analysis confirmed the alloy composition as [Si-0.522, Fe-0.981, Cu-0.585, Mn-0.098, Mg-0.481, Zn-0.266, Ti-0.017, Cr-0.052, Ni-0.032, with the balance being aluminum], verifying it as AA6063. The alloy's tensile strength was measured at 179 MPa, with a hardness of 75 HB. The workpiece selected for the welding trials had dimensions of 12 mm thickness, 102 mm width, and 203 mm length.

SS304, austenitic stainless steel, was used as the tool material for welding. This alloy, composed of 18% chromium and 8% nickel, is known for its excellent forming and welding properties, and does not require heat treatment as it does not harden through thermal processes [22]. Chemical analysis confirmed the tool material composition as [C-0.759, Si-0.464, Mn-1.36, P-0.0279, S-0.111, Cr-18.47, Mo-0.266, Ni-8.01, Co-0.218, Cu-0.355, with the balance being iron]. The tensile strength of SS304 was found to be 410 MPa, with a hardness of 200 HB. The welding tools were custom-designed with dimensions of 20 mm tool holder length, 40 mm tool shank length, 20 mm tool holder diameter, 40 mm tool shank diameter, and 12 mm tool pin diameter. Three tools were produced with varying pin lengths: tool 1 at 11 mm, tool 2 at 10 mm, and tool 3 at 11.5 mm.

The tools were manufactured using an EMCO Concept Turn 250 automatic turning machine, capable of a maximum speed of 6300 rpm, with a maximum diameter of 85 mm, a 250 mm swing, and 5.5 kW power. A carbide tool (VCGT 110302M SM-F) and a SVJCR/L-SH tool holder were used for machining. The welding process was conducted on a VMC 400 vertical milling center (manufactured by Parishudh Machine Ltd) with 11.5 kW spindle power, a spindle speed of 6000 rpm, and a table size of 900 mm x 450 mm, as shown in Fig. 1.

2.2. Experimentation plan

In this study, the welding settings spindle speed (*SS*), tool pin length (*TPL*), and tool pin shoulder rise (*TPSR*) were selected based on prior research [8]. Extensive trials, over 40 in total, were conducted to determine the appropriate parameter ranges by keeping traversing speed constant at 17 mm/min. The finalized levels for *SS*, *TPL*, and *TPSR* were 900, 1000, and 1100 rpm; 10, 11, and 11.5 mm; and 0.08, 0.18, and 0.28 mm, respectively. Using the full factorial method, 27 samples were required, but by applying the L9 orthogonal array, only 9 samples were necessary.

Experiments were performed, and the data generated were used to develop mathematical models through an artificial neuro-fuzzy inference system (ANFIS) and a multiple variable regression model (MVRM). In addition to the original 27 samples, 9 additional samples were prepared with a *TPSR* of 0.05 mm, leading to a total of 36 friction stir welding (FSW) joints. From each joint, 5 tensile test samples were prepared, resulting in 180 samples overall. Tensile tests were conducted on all samples, and the results from each of the 36 FSW joints were tabulated in Table 1. The experiments were repeated as per the L9 array to optimize the process using Taguchi analysis [23].

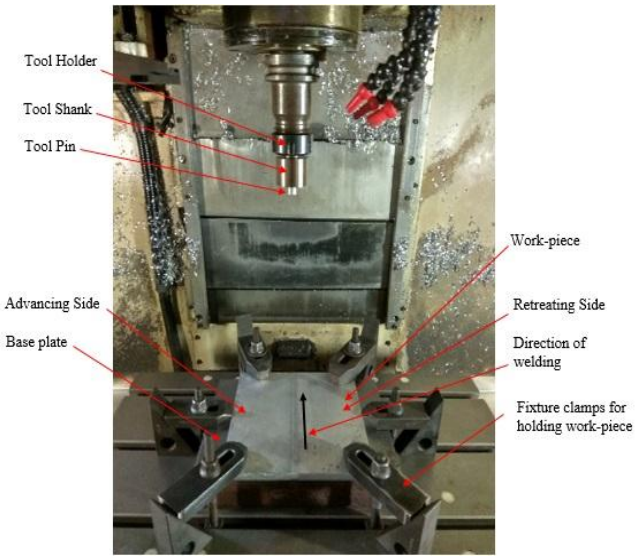

Fig. 1 Vertical milling center (VMC) setup

2.3. Tensile test

The tensile test specimens were prepared from the welded joints following ASTM-E8 specifications. The selected dimensions of the specimen are shown in Fig. 2. From each welded joint, five high-quality tensile test specimens were obtained. To prepare these specimens, the welded sample was cut into five sections, which were then processed into tensile test specimens. The cross-section of the cut weld sample is illustrated in Fig. 5. The tensile tests were conducted using a computerized universal testing machine (UTM) with a capacity of 100 tons, and the results are presented in Table 1.

In addition to testing the material's performance, such as environmental degradation and welding qualification, microstructural analysis was employed, which is a common approach in failure investigations [24]. This involves dividing the samples into smaller pieces and analyzing their basic components, from simple grain sizes to complex structures. This analysis provides critical insights into potential issues and reveals how processes like welding and machining affect the material's microstructure [25]. In this study, a metallurgical microscope with an image analyzer was used to obtain micrographs.

Table 1

Experimental data

S. No.	Spindle speed *SS*, rpm	Tool pin length *TPL*, mm	Tool pin shoulder rise *TPSR*, mm	Tensile strength *TS*, MPa
1	900	10	0.05	9.2
2	900	10	0.08	13.8
3	900	10	0.18	44.2
4	900	10	0.28	8.2
5	900	11	0.05	82.1
6	900	11	0.08	97.6
7	900	11	0.18	104.4
8	900	11	0.28	92.4
9	900	11.5	0.05	59.3
10	900	11.5	0.08	14.7
11	900	11.5	0.18	16.7
12	900	11.5	0.28	10.5
13	1000	10	0.05	15.5
14	1000	10	0.08	19.6
15	1000	10	0.18	59.3
16	1000	10	0.28	11.1
17	1000	11	0.05	124.4
18	1000	11	0.08	145.7
19	1000	11	0.18	149.6
20	1000	11	0.28	104.6
21	1000	11.5	0.05	77.7
22	1000	11.5	0.08	17.9
23	1000	11.5	0.18	25.1
24	1000	11.5	0.28	21.4
25	1100	10	0.05	19.2
26	1100	10	0.08	14.9
27	1100	10	0.18	49.7
28	1100	10	0.28	10.6
29	1100	11	0.05	91.4
30	1100	11	0.08	121.8
31	1100	11	0.18	120.3
32	1100	11	0.28	104.6
33	1100	11.5	0.05	65.4
34	1100	11.5	0.08	16.3
35	1100	11.5	0.18	18.2
36	1100	11.5	0.28	13.6

The tool dimensions used in the welding process were also crucial. The tool holder length (*A*) was 20 mm, the tool shank length (*B*) was 40 mm, and the tool pin lengths (*C*) for the three tools were 10 mm, 11 mm, and 11.5 mm, respectively. The tool shank diameter (*D*) was 40 mm, the tool holder diameter (*E*) was 20 mm, and the tool pin diameter (*F*) was 12 mm.

2.4. Taguchi method

In general, experiments are resource-intensive, requiring significant time, infrastructure, diagnostic instruments, personnel, and materials. Increased experimentation often leads to more waste production, resulting in greater resource consumption. These inefficiencies are known as "loss functions," as described by the renowned academician Taguchi, who linked such losses to deviations from the ideal mean.

The Taguchi method is widely used to minimize these inefficiencies. It begins by identifying the critical function or response variables and then selecting the objective function, commonly referred to as the signal-to-noise *(S/N)* ratios. The Taguchi method employs three types of

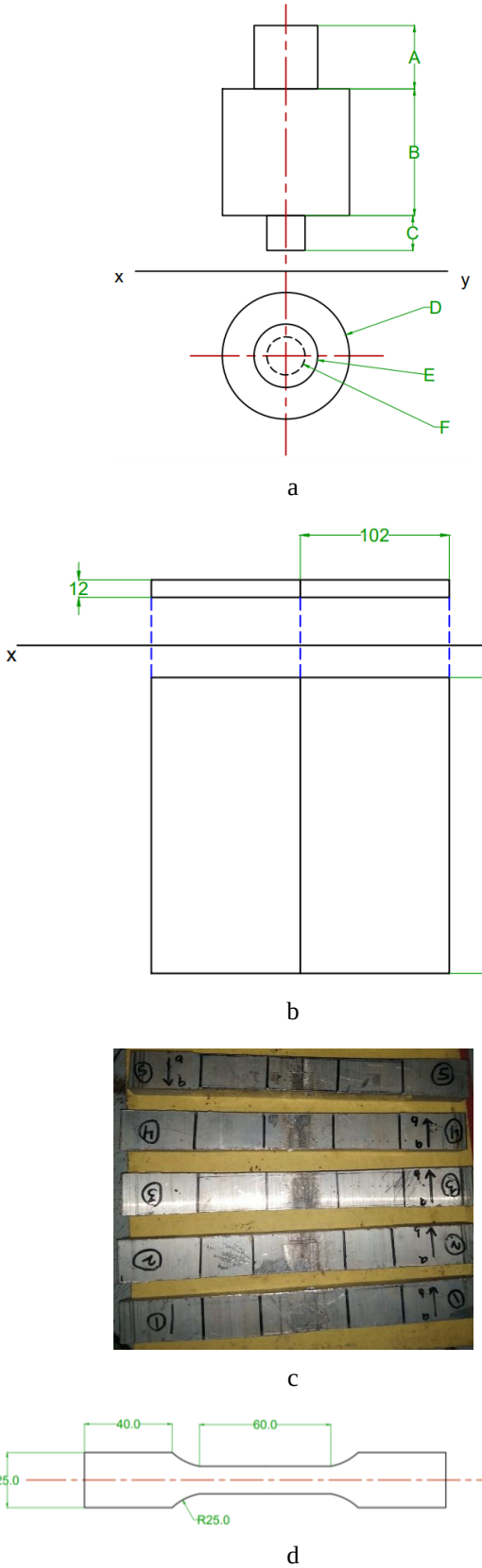

Fig. 2 Tool drawing (a), weld specimen drawing (b), weld sample cut into 5 pieces (c) and tensile test specimen (d)

S/N ratios to optimize performance: "smaller-the-better", "larger-the-better", and "nominal-the-best", each applied based on the nature of the desired outcome:

S/N ratio, smaller the better, $\eta_s = -10 log_{10} \frac{1}{n} \sum_{i=1}^{n} y_i^2$,

S/N ratio, larger the better, $\eta_s = -10\log_{10}\frac{1}{n}\sum_{i=1}^{n}\frac{1}{y_i^2}$,

S/N ratio, nominal the best, $\eta_s = -10\log_{10}\sigma^2$.

Here, n is the number of experiments conducted, y is the mean value of outputs, y_i is the i^{th} observed value of the output and σ is the standard deviations [26].

The parameters for the welding process were optimized using the Taguchi technique to achieve high product quality at an optimal cost [27]. Key factors influencing the tensile strength, including the tool's rotational speed, pin length, and tool pin shoulder rise, were identified as critical process parameters. The welding experiments were carried out using a vertical milling center (VMC) in line with the experimental design, and tensile tests were performed on the resulting joints.

To refine the process and determine the optimal tensile strength [8] achievable with the selected parameters, the Taguchi analysis was applied using the "larger-the-better" criterion. The resulting optimization curve is shown in Fig. 3. This approach ensured that the process was fine-tuned to yield the best tensile strength based on the chosen parameter values.

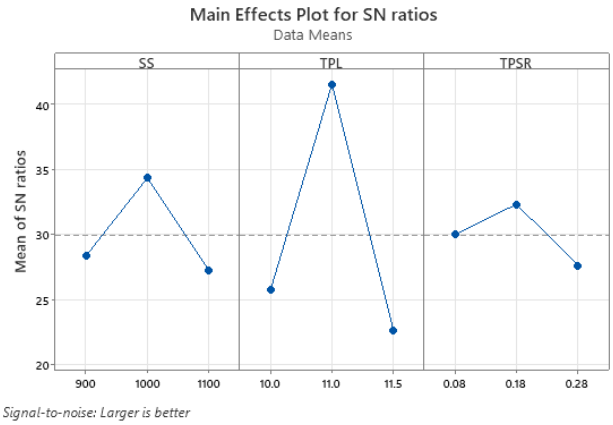

Fig. 3 *S/N* ratios plot

2.5. ANOVA results

The impact of input parameters on the output (tensile strength) was analyzed using ANOVA. Table 2 presents the results with a 95% confidence level and a 5% significance level. The F-values and percentage contribution ratio (PCR) in the table highlight the significance of each variable. Higher F-values indicate a stronger influence of the controlling factors on the outcome [28].

Table 2

ANOVA results

Source	DF	Seq SS	Adj SS	Adj MS	F	P	PCR, %
SS	2	88.15	88.15	44.08	2.42	0.292	11.36
TPL	2	617.89	617.89	308.95	16.98	0.056	79.65
TPSR	2	33.34	33.34	16.67	0.92	0.522	4.30
Residual Error	2	36.38	36.38	18.19	-	-	-
Total	8	775.77	-	-	-	-	-

The ANOVA results revealed that the tool pin length, spindle speed, and tool pin shoulder rise had the most significant impact on tensile strength, with contribution ratios of 79.65%, 11.36%, and 4.30%, respectively. These findings demonstrate the dominant role of tool pin length in determining weld quality, followed by spindle speed and tool pin shoulder rise.

2.6. Multiple variable regression model

To ascertain the relationship between the process variables, the multiple reversions approach is used. Eqs. 1-4 show multiple models for regression equations with three input parameters, including linear, quadratic, interaction, and complete models. The linear equation is given by

$$y = p_0 + p_1x_1 + p_2x_2 + p_3x_3 , \quad (1)$$

quadratic equation is given by

$$y = p_0 + p_1x_1 + p_2x_2 + p_3x_3 + p_4x_1^2 + p_5x_2^2 + p_6x_3^2 , \quad (2)$$

interaction equation is given by,

$$y = p_0 + p_1x_1 + p_2x_2 + p_3x_3 + p_4x_1x_2 + p_5x_1x_3 + p_6x_2x_3 , \quad (3)$$

second order equation (full model) is given by

$$y = p_0 + p_1x_1 + p_2x_2 + p_3x_3 + p_4x_1^2 + p_5x_2^2 + p_6x_3^2 + p_7x_1x_2 + p_8x_1x_3 + p_9x_2x_3 . \quad (4)$$

Here, y is criterion variable, x_1, x_2 and x_3 are predictor variable, p_0, p_1, p_2, p_3, p_4, p_5, p_6, p_7, p_8 and p_9 are coefficients [11]. The coefficients are obtained through the regression analysis of the experimentally obtained data. The regression coefficients obtained are: $p_0 = -18392.58$, $p_1 = 2.63$, $p_2 = 3177.11$, $p_3 = 1132.12$, $p_4 = 0.00$, $p_5 = -147.83$, $p_6 = -1272.96$, $p_7 = 0.01$, $p_8 = 0.01$, $p_9 = -65.85$. The strength of material under tensile load was calculated using second order equation (full model) was 114.33 MPa.

2.7. ANFIS modelling

The process was modeled using a mathematical tool, ANFIS (Artificial Neuro-Fuzzy Inference System), to predict tensile strength based on experimental data. The full factorial experimental results were used to create the Fuzzy Inference System (FIS) for the model [28]. A hybrid optimization technique, utilizing 100 epochs and a tolerance of 0.001, was applied to develop the FIS. Gaussian membership functions were selected for the inputs, while a linear function was chosen for the output.

After generating the FIS, the model was tested using approximately 33% of the experimental data. A graph was plotted to compare the predicted tensile strength values with the experimental input. The training process, using 27 fuzzy rules, was completed at the second epoch, with training and testing errors calculated as 11.6049 and 9.7186, respectively. The figures (Fig. 4, a-c) illustrate the tensile strength variations with changes in spindle speed (*SS*), tool

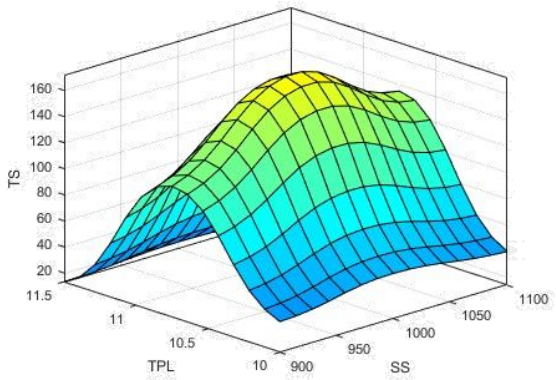

a

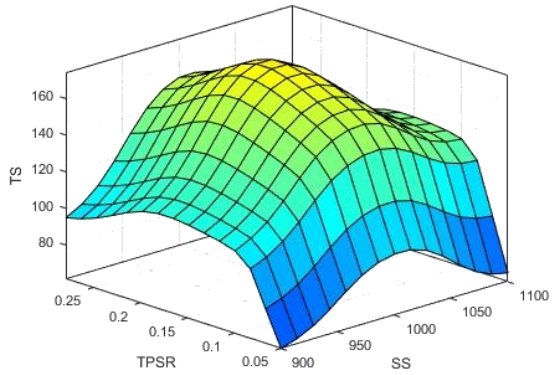

b

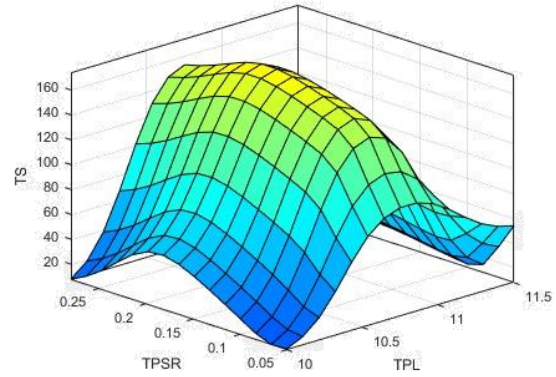

c

Fig. 4 Plot of *TS* with change in: a – *TPL* vs *SS*, b – *TPSR* vs *SS* and c – *TPSR* and *TPL*

pin length (*TPL*), and tool pin shoulder rise (*TPSR*), showing how different parameter combinations influence the output.

3. Results and Discussions

Trials were conducted to evaluate the strength of the welded joints under tensile load. Samples were prepared using both full factorial and DoE methods, with the cross-section of the weld shown in Fig. 5. Taguchi analysis was performed to determine the optimal tensile strength, and ANOVA results revealed that tool pin length *(TPL)* with a percentage contribution ratio (PCR) of 79.65%, spindle speed *(SS)* with a PCR of 11.36%, and tool pin shoulder rise *(TPSR)* with a PCR of 4.3% significantly impacted the joint's tensile strength. The optimal tensile strength was

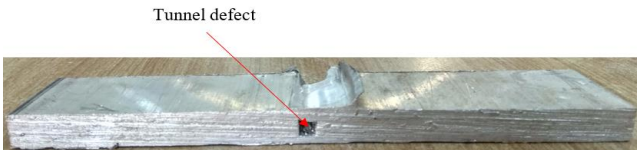

Fig. 5 Sectioned specimen with tunnel defect

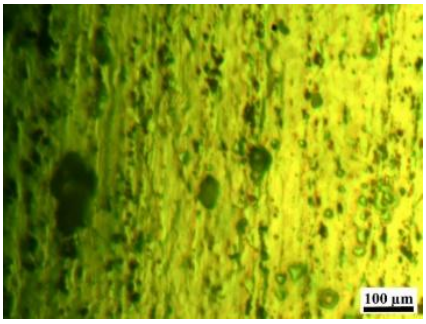

a

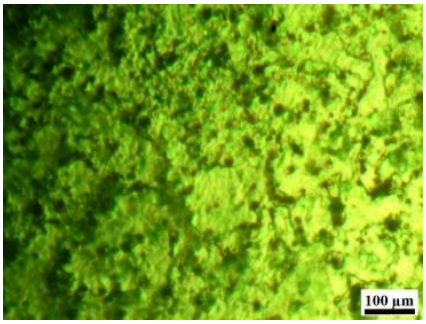

b

Fig. 6 Micrograph of: a – base material, b – HAZ at 400x

found at *SS*-1000 rpm, *TPL*-11 mm, and *TPSR*-0.18 mm. The experimentally obtained value was 149 MPa, while predictions from Minitab software and multiple variable regression produced values of 141.6 MPa and 114.33 MPa, respectively.

The ANFIS model was developed using experimental data, and the predicted tensile strength was 141 MPa. The graphs (Fig. 4) show the tensile strength variations with changes in *SS*, *TPL*, and *TPSR*. For example, (Fig. 4, a) illustrates that at 900 rpm, tensile strength increases with *TPL* up to 11 mm, after which it decreases. The strength peaks near *SS*-1000 rpm and *TPL*-11 mm. Similarly, (Fig. 4, b) shows that tensile strength increases with TPSR up to 0.18 mm and then declines, while (Fig. 4, c) highlights the interaction between *TPL* and *TPSR*, with maximum strength near *TPL*-11 mm and *TPSR*-0.18 mm.

In developing a method for welding 12 mm thick AA6063 aluminum plates, tool pin shoulder rise emerged as a critical parameter for achieving sound welds. Microstructural analysis using an image analyzer at 400x magnification (Fig. 6, a-b) showed a dendritic structure with no signs of slag inclusion or porosity, confirming complete fusion and a crack-free weld bead zone. Hardness values of 51 HV and 49 HV were recorded for the base material and heat-affected zone, respectively.

The tensile strength trends based on input parameters are illustrated in Figs. 7-9. These plots reveal that tensile strength peaks at *SS*-1000 rpm (Fig. 7), *TPL*-11 mm (Fig. 8). At *TPSR*-0.18 mm (Fig. 9) the variation in tensile strength observed is minimal.

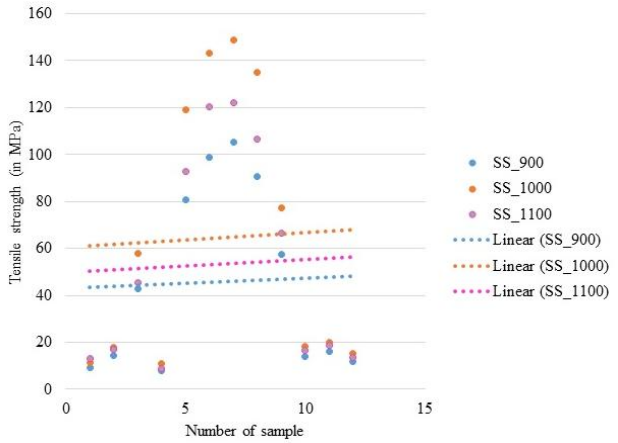

Fig. 7 Plot of tensile strength with variation in the spindle speed

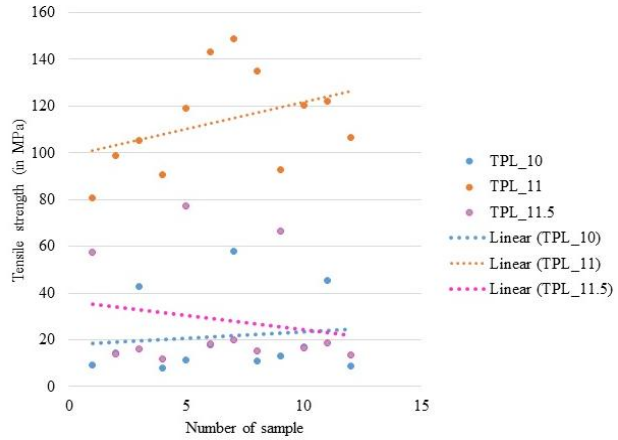

Fig. 8 Plot of tensile strength with variation in the tool pin length

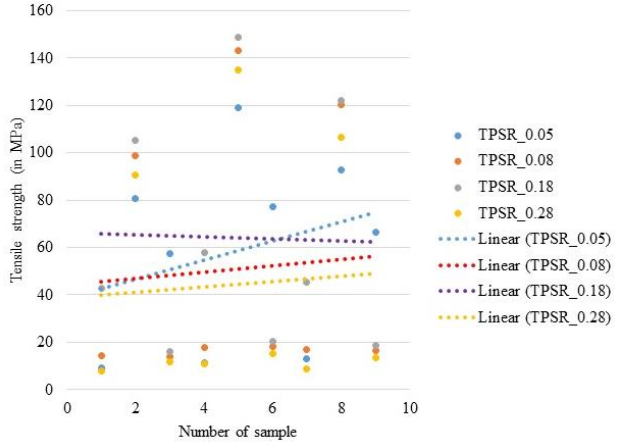

Fig. 9 Plot of tensile strength with variation in the tool pin shoulder rise

4. Conclusions

The experimental data were used to optimize the process via Minitab software, and a mathematical model was developed using ANFIS. According to ANOVA results, tool pin length *(TPL)* had the highest impact on tensile strength at 79.65%, followed by spindle speed *(SS)* at 11.36%, and tool pin shoulder rise *(TPSR)* at 4.3%. Taguchi analysis, supported by experimental data and figures (Fig. 6-8), identified the optimal values for *SS*, *TPL*, and *TPSR* as 1000 rpm, 11 mm, and 0.18 mm, respectively. The Taguchi method predicted an optimized tensile strength of 149 MPa, while Minitab software estimated 141.6 MPa. The multiple variable regression equation yielded 114.33 MPa, and the ANFIS model predicted 141 MPa. Deviations from the experimental tensile strength were 4.97%, 23.27%, and 5.37% for Minitab, regression, and ANFIS models, respectively.

Micrograph analysis confirmed sound welding in all 36 specimens, with proper fusion and no visible defects near the weld bead. The lower tensile strength observed in some specimens was likely due to tunnel defects, as shown in Fig. 5. Despite Taguchi analysis indicating that *TPL* was the most significant factor influencing welded joint strength, the *TPSR*, though least significant, proved essential during experimental work for successful FSW joining of the 12 mm thick AA6063. Hardness values of the base material and heat-affected zone were consistent across all FSW specimens, at 51 HV and 49 HV, respectively.

Statements & Declarations

Funding: The authors declare that no funds, grants, or other support were received during the preparation of this manuscript.

Competing Interests: The authors have no relevant financial or non-financial interests to disclose.

Conflict of interest: The authors declare that there is no conflict of interest.

Note: Any further details can be accessed through mail (mail to, deepmish981@gmail.com or ravp077@gmail.com).

References

1. **Koilraj M.; Sundareswaran, V.; Vijayan, S.; Koteswara Rao, S. R.** 2012. Friction stir welding of dissimilar aluminum alloys AA2219 to AA5083 - Optimization of process parameters using Taguchi technique 42: 1-7. https://doi.org/10.1016/j.matdes.2012.02.016.
2. **Li W.; Patel V.** 2022. Solid State Welding for Fabricating Metallic Parts and Structures, Encyclopedia of Materials: Metals and Alloys 4: 246-259. https://doi.org/10.1016/B978-0-12-819726-4.00012-0.
3. Chapter 14 - Friction Stir Welding. 2009. Handbook of Plastics Joining (Second Edition), Editor(s): M. J. Troughton: 131-134. https://doi.org/10.1016/B978-0-8155-1581-4.50016-0.
4. **Gibson, B. T.; Lammlein, D. H.; Prater, T. J.; Longhurst, W. R.; Cox, C. D.; Ballun, M. C.; Dharmaraj, K. J.; Cook, G. E.; Strauss, A. M.** 2014. Friction stir welding: Process, automation, and control, Journal of Manufacturing Processes 16(1): 56–73. https://doi.org/10.1016/j.jmapro.2013.04.002.
5. **Majeed, T.; Wahid, M. A.; Alam, M. N.; Mehta, Y.; Siddiquee, A. N.** 2021. Friction stir welding: A sustainable manufacturing process, Materials Today: Proceedings 46: 6558–6563. https://doi.org/10.1016/j.matpr.2021.04.025.
6. **Liu, H. J.; Fujii, H.; Maeda, M.; Nogi, K.** 2003. Tensile properties and fracture locations of friction-stir-welded joints of 2017-T351 aluminum alloy, Journal of Materials Processing Technology 142(3): 692–696. https://doi.org/10.1016/S0924-0136(03)00806-9.

7. **Janeczek, A.; Tomków, J.; Fydrych, D.** 2021. The Influence of Tool Shape and Process Parameters on the Mechanical Properties of AW-3004 Aluminium Alloy Friction Stir Welded Joints, Materials. 14(12): 3244. https://doi.org/10.3390/ma14123244.
8. **Mishra, D.; Prasad, R. S.; Kumar, S.** 2021. ANFIS Model to Predict Effect of Tool Pin Length and Position on Tensile Strength of Friction Stir Welded Joint, Welding International 35(1–3): 24-33. https://doi.org/10.1080/09507116.2021.1917972.
9. **Silva, A. C. F.; Braga, D. F. O.; de Figueiredo, M. A. V.; Moreira, P. M. G. P.** 2015. Ultimate tensile strength optimization of different FSW aluminium alloy joints, The International Journal of Advanced Manufacturing Technology 79: 805–814. https://doi.org/10.1007/s00170-015-6871-2.
10. **Dhas, J. E. R.; Dhas, S. J. H.** 2012. A review on optimization of welding process, Procedia Engineering 38: 544-554. https://doi.org/10.1016/j.proeng.2012.06.068.
11. **Binoj, J. S.; Manikandan, N.; Thejasree, P.; Varaprasad, K. C.; Sai, N. P.; Manideep, M.** 2021. Machinability studies on wire electrical discharge machining of Nickel alloys using multiple regression analysis, Materials Today – Proceedings 39: 155-159. https://doi.org/10.1016/j.matpr.2020.06.407.
12. **Zhang, H.; Liu, H.** 2013. Mathematical model and optimization for underwater friction stir welding of a heat-treatable aluminum alloy, Materials and Design 45: 206–211. https://doi.org/10.1016/j.matdes.2012.09.022.
13. **Lakshminarayanan, A. K.; Balasubramanian V.** 2008. Process parameters optimization for friction stir welding of RDE-40 aluminium alloy using Taguchi technique, Transactions of Nonferrous Metals Society of China (English Ed.) 18(3): 548-554. https://doi.org/10.1016/S1003-6326(08)60096-5.
14. **Shunmugasundaram M.; Kumar A.; Sankar L.; Sivasankar S.** 2020. Optimization of process parameters of friction stir welded dissimilar AA6063 and AA5052 aluminum alloys by Taguchi technique, Mater Today Proc. 27: 871–876. https://doi.org/10.1016/j.matpr.2020.01.122.
15. **Jagadish; Bhowmik, S.; Ray, A.** 2016. Prediction and optimization of process parameters of green composites in AWJM process using response surface methodology, The International Journal of Advanced Manufacturing Technology 87(5–8): 1359–1370. https://doi.org/10.1007/s00170-015-8281-x.
16. **Rajkumar, T.; Radhakrishnan, K.; Rajaganapathy C.; Jani, S. P.; Salmaan, N. U.** 2022. Experimental Investigation of AA6063 Welded Joints Using FSW, Advances in Materials Science and Engineering 2022: 4174210. https://doi.org/10.1155/2022/4174210.
17. **Shehabeldeen, T. A.; Elaziz, M. A.; Elsheikh, A. H.; Zhou J.** 2019. Modeling of friction stir welding process using adaptive neuro-fuzzy inference system integrated with harris hawks optimizer, Journal of Materials Research and Technology. 8(6): 5882–5892. https://doi.org/10.1016/j.jmrt.2019.09.060.
18. **Dewan, M. W.; Huggett, D. J.; Liao, T. W.; Wahab, M. A.; Okeil, A. M.** 2016. Prediction of tensile strength of friction stir weld joints with adaptive neuro-fuzzy inference system (ANFIS) and neural network, Materials and Design 92: 288-299. https://doi.org/10.1016/j.matdes.2015.12.005.
19. **Shanavas, S.; Dhas, J. E. R.** 2017. ANFIS modeling of friction stir weld parameters, 2016 International Conference on Control, Instrumentation, Communication and Computational Technologies (ICCICCT): 772-777. https://doi.org/10.1109/ICCICCT.2016.7988056.
20. **Vijayan, D.; Rao, V. S.** 2016. Parametric optimization of friction stir welding process of age hardenable aluminum alloys − ANFIS modeling, Journal of Central South University 23(8): 1847–1857. https://doi.org/10.1007/s11771-016-3239-1.
21. Aalco Metals, Aluminium Alloy 6063. 2009. 9-11. https://www.aalco.co.uk/datasheets/Aalco-Metals-Ltd_Aluminium-Alloy-6063-0-Extrusions_160.pdf.ashx.
22. Stainless Steel Grade Datasheets, Publ. by Atlas Steels Tech. Dep. 2013. Available at: https://www.atlassteels.com.au/documents/Atlas Grade datasheet - all datasheets rev Aug 2013.pdf.
23. **Jagadeesha, C. B.** 2017. The combined theoretical and experimental approach to arrive at optimum parameters in friction stir welding, Journal of the Mechanical Behavior of Materials 26(3-4): 133–138. https://doi.org/10.1515/jmbm-2017-0022.
24. **Huang, H. Y.; Kuo, I. C.; Zhang C. W.** 2018. Friction-stir welding of aluminum alloy with an iron-based metal as reinforcing material, Science and Engineering of Composite Materials 25(1): 123–131. https://doi.org/10.1515/secm-2016-0065.
25. **He, W.; Liu, J.; Hu, W.; Wang, G.; Chen, W.** 2019. Controlling residual stress and distortion of friction stir welding joint by external stationary shoulder, High Temperature Materials and Processes 38(2019): 662-671. https://doi.org/10.1515/htmp-2019-0005.
26. **Yuvaraj, K. P.; Varthanan, P. A.; Haribabu, L.; Madhubalan, R.; Boopathiraja, K. P.** 2021. Optimization of FSW tool parameters for joining dissimilar AA7075-T651 and AA6061 aluminium alloys using Taguchi Technique, Materials Today - Proceedings 45(2): 919-925. https://doi.org/10.1016/j.matpr.2020.02.942.
27. **Ross, P. J.** 2017. Taguchi Techniques for Quality Engineering. 2nd Edition. McGraw-Hill. 350p.
28. **Prasad, R. S.; Mishra, D.; Swarnkar, J.; Kumawat, O.; Pandey, M.; Gupta, A.** 2022. Fatigue analysis of SAE8620: Synergistic effect of thermal treatments and surface roughness, Advances in Materials and Processing Technologies 9(4): 2042-2058. https://doi.org/10.1080/2374068X.2022.2152594.

D. Mishra, R. S. Prasad, S. Kumar

OPTIMIZATION OF TENSILE STRENGTH IN AA6063 FRICTION STIR WELDS USING ANOVA AND ANFIS: A STATISTICAL ANALYSIS OF PROCESS PARAMETERS

S u m m a r y

Friction stir welding (FSW) is an effective technique for joining aluminum alloys like AA6063, known for their strength and durability. This research focuses on optimizing FSW process parameters to enhance the tensile strength of 12 mm thick AA6063 joints, combining experimental research with statistical analysis and predictive modeling. Key process variables spindle speed, tool pin length, and tool pin shoulder rise were evaluated through experiments designed using a full factorial approach and L9 orthogonal array. ANOVA (Analysis of Variance) was employed to assess the significance and impact of these parameters on tensile strength. Results revealed that tool pin length had the greatest influence, with a percentage contribution ratio (PCR) of 79.65%. Predictive models were developed using multiple variable regression and ANFIS (Artificial Neuro-Fuzzy Inference System), yielding tensile strength predictions with percent errors of 23.27% and 6.04%, respectively. This study highlights the importance of optimizing process parameters, particularly tool pin length, to achieve higher tensile strength in FSW joints, providing valuable insights for the welding of aluminum alloys.

Keywords: tool pin length, tool pin shoulder rise, friction stir welding, Taguchi, ANOVA, ANFIS.

Received May 3, 2023
Accepted December 16, 2024